Communication in Physical Sciences, 2026, 13(9): 1504-1521

Study of Performance and Radiation-Shielding Properties of Samarium-Doped Calcium Sulfur-Phosphate Glasses for Enhanced Ionizing Radiation Protection

Tanimu Hussaini*, Sadiq Abubakar Dalhatu, Dauda Abubakar, Auwal Baballe, Yawale Abubakar Ibrahim, Mohammed Auwal Yusuf, Haruna Saleh, Mohammed Rabiu, Nafisa Musa, and Adamu Adamu

Received: 02 June 2026/Accepted: 20 August 2026/Published: 27 August 2026
https://doi.org/10.4314/cps.v13i9.7

Abstract: *The present study investigated the gamma-radiation shielding properties of samarium oxide (Sm_2O_3)-modified calcium sulfate–phosphate glasses with nominal composition 20CaSO4+(80−x)P2O3+ xSm2O320CaSO₄+(80-)P_2O_3+xSm_2O₃, where x=0.50–2.50x=0.50–2.50 mol%. The mass attenuation coefficient (MAC), linear attenuation coefficient (LAC), half-value layer (HVL), mean free path (MFP), and effective atomic number (ZeffZ_{\mathrm{eff}}) were evaluated over photon energies ranging from 0.015 to 15 MeV using the Phy-X/PSD computational platform. The results demonstrated a strong energy- and composition-dependent shielding response. At 0.015 MeV, the MAC increased from 11.990 cm^2/g for S1 to 58.518 cm^2/g for S4, while the corresponding LAC values increased from 43.404 to 182.576 cm^{-1}. At 15 MeV, the LAC values were 0.083, 0.096, 0.129 and 0.132 cm^{-1} for S1–S4, respectively. The HVL increased with photon energy, reaching 8.377 cm for S1 and 5.392 cm for S4 at 15 MeV, indicating improved attenuation by the Sm_2O_3-rich composition. Similarly, the MFP at 0.015 MeV decreased from 0.013 cm for S1 to 0.005 cm for S4, confirming the enhanced probability of photon interaction in the Sm_2O_3-containing glass. The calculated ZeffZ_{\mathrm{eff}} values further showed substantial compositional differences, with S4 exhibiting values of 27.90 at 0.347 MeV and 31.99 at 15 MeV, compared with 11.96 and 12.80, respectively, for S1. Overall, the results indicate that increasing Sm_2O_3 content substantially improves the photon attenuation characteristics of the investigated glasses, with S4 demonstrating the most promising shielding performance for gamma-radiation protection applications.*

Keyword: Calcium Sulfur-Phosphate, Glasses, Samarium, ionizing radiation, shielding application

Tanimu Hussaini
Department of Physics, Sa'adu Zungur University, Bauchi State, Nigeria.
Email: tanimuhussaini53@gmail.com

Sadiq Abubakar Dalhatu
Department of Physics, Sa'adu Zungur University, Bauchi State, Nigeria.
Email: adgambaki@gmail.com
https://orcid.org/0000-0002-7557-4530

Dauda Abubakar
Department of Physics, Sa'adu Zungur University, Bauchi State, Nigeria.
Email: dabubakar19@yahoo.com

Auwal Baballe
Department of Physics, Sa'adu Zungur University, Bauchi State, Nigeria.
Email: abuumusaab@gmail.com

Yawale Abubakar Ibrahim
Department of Science Laboratory Technology, Federal Polytechnic Kaltungo, Gombe State, Nigeria.

Corresponding author Email: tanimuhussaini53@gmail.com

Email: **AbubakarIbrahimyawale@fedpolyklt.edu.ng**
https://orcid.org/0009-0002-0963-5021

Mohammed Auwal Yusuf
Department of Physics, Abubakar Tafawa Balewa University, Bauchi, Nigeria.
Email: aymohammed@atbu.edu.ng
https://orcid.org/0000-0003-0767-8845

Haruna Saleh
Department of Physics, Sa'adu Zungur University, Bauchi State, Nigeria.
Email: atfashionandstyleschool@gmail.com

Mohammed Rabiu
Department of Science Laboratory Technology, Federal Polytechnic Kaltungo, Gombe State, Nigeria.
Email: mohammedrabiu@fedpolyklt.edu.ng
https://orcid.org/0009-0008-5016-7358

Nafisa Musa
Department of Science Lab.Tech. Federal Polytechnic Kaltungo Gombe State Nigeria
Email: nafisamusa@fedpolyklt.edu.ng
https://orcid.org/0009-0000-2649-5281

Adamu Adamu
[1]Department of Physics, Sa'adu Zungur University Bauchi State Nigeria
Email: adamuadamumad@gmail.com

1.0 Introduction

The increasing use of ionizing radiation, particularly X-rays and gamma photons, in diagnostic radiography, radiotherapy, nuclear technology, industrial inspection, and other technological applications has intensified the need for effective, reliable, and environmentally sustainable radiation-shielding materials. Although ionizing radiation has important medical, industrial, and scientific applications, excessive or prolonged exposure can cause cellular and molecular damage, including DNA injury, thereby increasing the risk of adverse biological effects (Akram & Chowdhury, 2023; Auwal *et al.*, 2022). Consequently, radiation protection relies on controlling exposure through time, distance, and shielding, with shielding becoming particularly important in situations where exposure duration and distance cannot be adequately controlled (Frane & Bitterman, 2023; Kim *et al.*, 2018).The attenuation of photons in a shielding material is strongly dependent on photon energy and the elemental composition of the absorber. At relatively low photon energies, photoelectric absorption is the dominant interaction mechanism and attenuation is strongly influenced by atomic number; at intermediate energies, Compton scattering becomes increasingly important, whereas pair production becomes significant at higher photon energies above its threshold. Consequently, shielding performance is commonly assessed using parameters such as the mass attenuation coefficient (MAC), linear attenuation coefficient (LAC), half-value layer (HVL), mean free path (MFP), and effective atomic number (Z_eff), which collectively describe the ability of a material to attenuate incident photons (Arul Raja Sekaran *et al.*, 2024; Hanfi *et al.*, 2023). Among the available shielding materials, glass systems have attracted considerable attention because their composition can be systematically tailored to modify density, atomic number, structural characteristics, and photon-interaction mechanisms while maintaining optical transparency and relatively simple fabrication routes (Ige *et al.*, 2023; Geidam *et al.*, 2022). Recent investigations have demonstrated that compositional modification of phosphate- and calcium-containing glasses can substantially influence their radiation attenuation characteristics. For example, calcium phospho-silicate glasses containing different proportions of MgO exhibited composition-dependent changes in their linear attenuation coefficients, with enhanced attenuation observed at lower photon energies and with increasing MgO incorporation (Arul Raja Sekaran *et al*., 2024). Similarly, Hanfi *et al*. (2023) reported that increasing As_2O_3 concentration in B_2O_3–As_2O_3 glass ceramics increased the linear attenuation coefficient and improved the shielding performance, particularly in the low-energy gamma-ray region. Calcium sulfate–phosphate glasses are particularly promising because their composition provides opportunities for structural and compositional modification through the incorporation of suitable network modifiers and rare-earth oxides. Recent work on calcium sulfate ultra-phosphate glasses has shown that rare-earth modification can produce substantial changes in photon attenuation. Barde *et al*. (2026) investigated calcium sulfate ultra-phosphate glasses containing different concentrations of Dy_2O_3 and reported that increasing Dy_2O_3 content enhanced the density, mass attenuation coefficient, and linear attenuation coefficient while reducing the half-value layer, tenth-value layer, and mean free path. The highest Dy_2O_3-containing composition exhibited the most favorable overall shielding characteristics, demonstrating that rare-earth incorporation can be an effective strategy for improving the radiation attenuation performance of calcium sulfur-phosphate glass matrices (Barde *et al*., 2026).

Although lead-based glasses provide effective shielding, their toxicity and environmental impacts necessitate safer alternatives (Hila *et al*., 2022; More *et al*., 2021). Consequently, increasing attention has been directed toward lead-free glass systems containing high-atomic-number metal oxides and rare-earth ions as compositional modifiers. Rare-earth incorporation can alter glass density, network structure, and photon-interaction probability, thereby influencing key shielding parameters such as the mass attenuation coefficient (MAC), linear attenuation coefficient (LAC), half-value layer (HVL), and mean free path (MFP). In particular, samarium oxide (Sm_2O_3) is a promising modifier because its incorporation can increase the effective interaction probability of photons within a glass matrix. Recent work on Sm_2O_3-doped photopolymer composites demonstrated that increasing Sm_2O_3 concentration significantly increased both MAC and LAC while reducing HVL, with the highest Sm_2O_3-containing composition showing the strongest attenuation performance (Zaynal *et al*., 2026). These findings suggest that Sm_2O_3 incorporation may provide an effective route for enhancing the photon-shielding performance of lead-free materials.Despite these advances, the shielding behavior of calcium sulfur-phosphate glasses remains insufficiently explored with respect to the systematic incorporation of different rare-earth oxides, particularly Sm_2O_3. Although Barde *et al*. (2026) demonstrated that Dy_2O_3 incorporation can enhance the density and photon attenuation characteristics of calcium sulfate ultra-phosphate glasses, the effect of Sm_2O_3 concentration on the attenuation behavior of this glass family has not been adequately established. Moreover, the energy-dependent response of Sm_2O_3-modified calcium sulfur-phosphate glasses across a broad photon-energy interval, together with the associated variations in MAC, LAC, HVL, MFP, and Z_{eff}, requires further investigation. This gap is important because different rare-earth ions may produce different compositional, density, and photon-interaction responses within a similar glass network. Therefore, systematic evaluation of Sm_2O_3 concentration is necessary to determine whether samarium incorporation can provide comparable or improved shielding performance within the calcium sulfur-phosphate matrix. Borate and sulphate glasses offer low melting temperature, transparency, and thermal stability (Auwal *et al.,* 2025; Sivasankara, 2022), suggesting opportunities for compositional engineering. Therefore, the aim of this study is to investigate the influence of Sm_2O_3 incorporation on the physical and photon-shielding properties of calcium sulfur-phosphate glasses. Glass compositions containing 1.0, 1.5, 2.0, and 2.5 mol% Sm_2O_3 were prepared using the melt-quenching technique, and their densities and photon attenuation characteristics were evaluated over the 0.015–15 MeV energy range. Specifically, the study evaluates the effects of Sm_2O_3 concentration on the mass attenuation coefficient, linear attenuation coefficient, half-value layer, mean free path, and effective atomic number to identify the composition with the most favorable photon-shielding performance. The significance of this study lies in providing experimental and theoretical evidence for the compositional optimization of transparent, lead-free glass materials for ionizing-radiation protection. Establishing the relationship between Sm_2O_3 concentration, density, and photon attenuation can provide useful information for the development of alternative shielding materials for medical, nuclear, industrial, and other radiation-related applications where conventional lead-based materials are undesirable because of their toxicity and environmental concerns. The findings may also provide a basis for comparison with other rare-earth-modified calcium sulfur-phosphate glasses and contribute to the broader development of compositionally tunable radiation-shielding materials.

2.0 Materials and Methods

2.1 Materials

The materials used for the preparation and radiation-shielding evaluation of the glasses included calcium sulfate ($CaSO_4$), phosphorus oxide (P_2O_3/P_2O_5; to be verified), and samarium oxide (Sm_2O_3). Phy-X/PSD software was used to calculate the photon-interaction and radiation-shielding parameters of the prepared glass compositions. The glass compositions investigated in this study are presented in Table 1.The author used the standard melt quenching technique to prepare the selected glasses. The weights of the raw materials were measured by a precision weighing balance. The mixed batch materials were then placed in an electric furnace and pre–heated to a temperature of 400 ºC for 30 minutes. The batches were then melted in an electric furnace at 1200 ºC for 1hour. The last step, the melt was quenched at room temperature by pouring on a stainless steel block

The density of each glass sample was determined using Archimedes' principle. The mass of the sample in air and its apparent mass when immersed in a liquid of known density were measured using a precision balance. The density of the glass was calculated using equation 1

$$Density(\rho) = \frac{m_a}{m_a - m_l}\rho_l \qquad (1)$$

where ρ is the density of the glass sample, mam_m_a is its mass in air, m_l is its apparent mass when immersed in the liquid, and ρ_l is the density of the immersion liquid.

2.2 Radiation Shielding Simulation

The radiation shielding parameters of the Sm_2O_3 Calcium Sulfur-Phosphate glasses system were computed by utilising user-friendly online Phy-X/PSD software developed by Sakar *et al*. (2020). The shielding parameters, such as mass attenuation coefficient (μ_m), linear attenuation coefficient (μ) coefficient half-value layer (HVL), effective atomic number *(Z_{eff})* were calculated in the energy range from 0.015 to 15 MeV.

PHY-X/PSD Software

Phy-X/PSD software, which was recently developed to determine the radiation shielding parameters of different materials, was used in the calculation. The calculation process was started by defining the chemical composition and the density of the material in the program. In the software, the material composition can be entered as mole fraction, as shown in *Fig.* 1. The parameters were determined in a wide energy range by selecting the energy sources (^{22}Na, ^{55}Fe, ^{60}Co, ^{109}Cd, ^{13}1I, ^{133}Ba, ^{137}Cs, ^{152}Eu, ^{241}Am and the K-shell energies of Cu, Rb, Mo, Ag, Ba and Tb elements). Lastly, the desired shielding parameters were determined by the software.

Table 1 The doped chemical composition 20$CaSO_4$ + (80-x) P_2O_3 +xSm_2O_3 with 0.50 ≤ x ≤ 2.50 mol % glass.

Glass Sample Code	$CaSO_4$ mol.%	(80-x)P_2O_3 Mol.%	xSm_2O_3 Mol.%	Density g/cm^3
S1	20	79.00	1.00	3.12
S2	20	78.5	1.50	3.62
S3	20	78.00	2.O0	4.12
S4	20	77.50	2.50	5.47

3.0 Results and Discussion

3.1 Radiation *Shielding Parameters*

The mass attenuation coefficient (MAC), μ/ρ\mu/\rho, represents the probability of photon interaction per unit mass thickness of the material and is expressed in cm² g⁻¹ The μ_m values for the glasses with composition 20$CaSO_4$ + (80-x)P_2O_3 +xSm_2O_3 with 0.50 ≤ x ≤ 2.50 mol % were obtained by utilizing the Phy-X/PSD software.

$$\mu_m = \mu\rho^{-1} = \sum_i w_i(\mu_m)_i \quad (1)$$

The variable w_i denotes the fraction of weight attributable to its constituent element.

Fig. 1 and Table 1 illustrate the MAC (cm^2/g) Variation with the photon energy for all the prepared glasses samples over the energy ranges (0.015 to 15 MeV).

The MAC of all the prepared samples (S1 – S4) is within the range of 11.990 – 58.518 cm^2/g at lower photon energy (E=0.015MeV). As shown in the Fig 2, the sample containing a higher amount of Sm_2O_3 exhibits the maximum value of MAC (58.518 cm^2/g) at a lower photon energy (E=0.015MeV) compared with the samples with a lower percentage of the dopant Sm_2O_3. Obviously, as the photon energy increases from 0.015 to 15MeV, the MAC shows a reduction in descending order across all the samples. This can be explained in terms of the absorption cross section in the low energies (photoelectric absorption, PE), intermediate energies (Compton scattering, CS) and high energies (pair production, PP) becomes predominant (Saddeek *et al*., 2020).

As shown in the Fig. 2, the sharp decrease in MAC values as photon energy increases can be attributed to (PE). At lower energy regions (E ≤ 0.4MeV) and high atomic number elements (Z) and is the most predominant cross section, such that PE ∝ $Z^4E^{-3.5}$ (Sayyed *et al.*, 2019). In contrast, as the photon energy increases at the energy region (0.4MeV < E< 3.9MeV), the Compton scattering CS cross section superseded PE interaction and became the major interaction mechanism (CS ∝ Z/E). In the higher energy region (E >1.0MeV) in which the Pair production cross section prevails, the value of the MAC becomes almost constant for all the samples. The investigated glasses exhibit an increasing trend of the MAC with varying amounts of Sm_2O_3 in the order of S1 > S2 > S3 > S4, and we observed that increase in density of the prepared samples (Table 2) correlates with the increasing value of the MAC.

Convincingly, the sample S4 demonstrates superior radiation attenuation efficiency based on its high MAC compared S1, S2 and S3 samples. Several researchers reported similar results for other glasses. Investigated the influence of addition of BaO radiation shielding properties of titano- Phosphate glass. The mass attenuation coefficient varies with BaO concentration. At a gamma photon energy of 0.015 MeV, the highest mass attenuation coefficient changes between 12.198 and 21.806 cm²/g. (Rammah *et al.,* 2022).

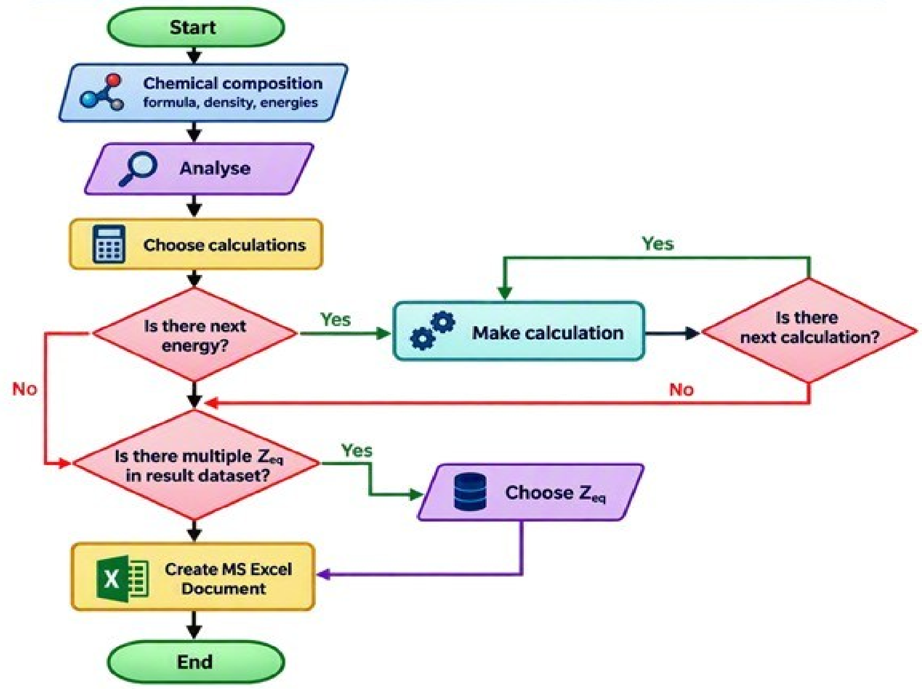

***Fig.* 1. Flow chart of the Phy-X/PSD online software (Sakar *et al.*, 2020).**

Table 2: MAC values of $20CaSO_4 + (80-x) P_2O_3 + xSm_2O_3$ with $0.50 \leq x \leq 2.50$ mol % glass system

Energy (MeV)	S_1	S_2	S_3	S_4
1.50E-02	11.990	12.921	13.833	58.518
2.00E-02	5.338	5.775	6.204	27.224
3.00E-02	1.767	1.916	2.062	9.232
4.00E-02	0.861	0.930	0.998	4.320
5.00E-02	1.068	1.278	1.485	11.653
6.00E-02	0.712	0.843	0.971	7.289
8.00E-02	0.404	0.465	0.524	3.457
1.00E-01	0.282	0.315	0.347	1.945
1.50E-01	0.176	0.186	0.197	0.716
2.00E-01	0.141	0.145	0.150	0.381
2.84E-01	0.115	0.116	0.118	0.203
3.00E-01	0.111	0.113	0.114	0.187
3.47E-01	0.104	0.105	0.106	0.153

4.00E-01	0.097	0.098	0.098	0.129
5.00E-01	0.087	0.088	0.088	0.103
6.00E-01	0.080	0.080	0.081	0.088
6.62E-01	0.077	0.077	0.077	0.082
8.00E-01	0.070	0.070	0.070	0.071
8.26E-01	0.069	0.069	0.069	0.070
1.00E+00	0.063	0.063	0.063	0.062
1.17E+00	0.058	0.058	0.058	0.056
1.33E+00	0.054	0.054	0.054	0.052
1.50E+00	0.051	0.051	0.051	0.049
2.00E+00	0.044	0.044	0.044	0.043
2.51E+00	0.039	0.039	0.039	0.040
3.00E+00	0.036	0.036	0.036	0.038
4.00E+00	0.032	0.032	0.032	0.036
5.00E+00	0.029	0.029	0.029	0.035
6.00E+00	0.027	0.027	0.028	0.035
8.00E+00	0.025	0.025	0.026	0.035
1.00E+01	0.024	0.024	0.024	0.036
1.50E+01	0.023	0.023	0.024	0.039

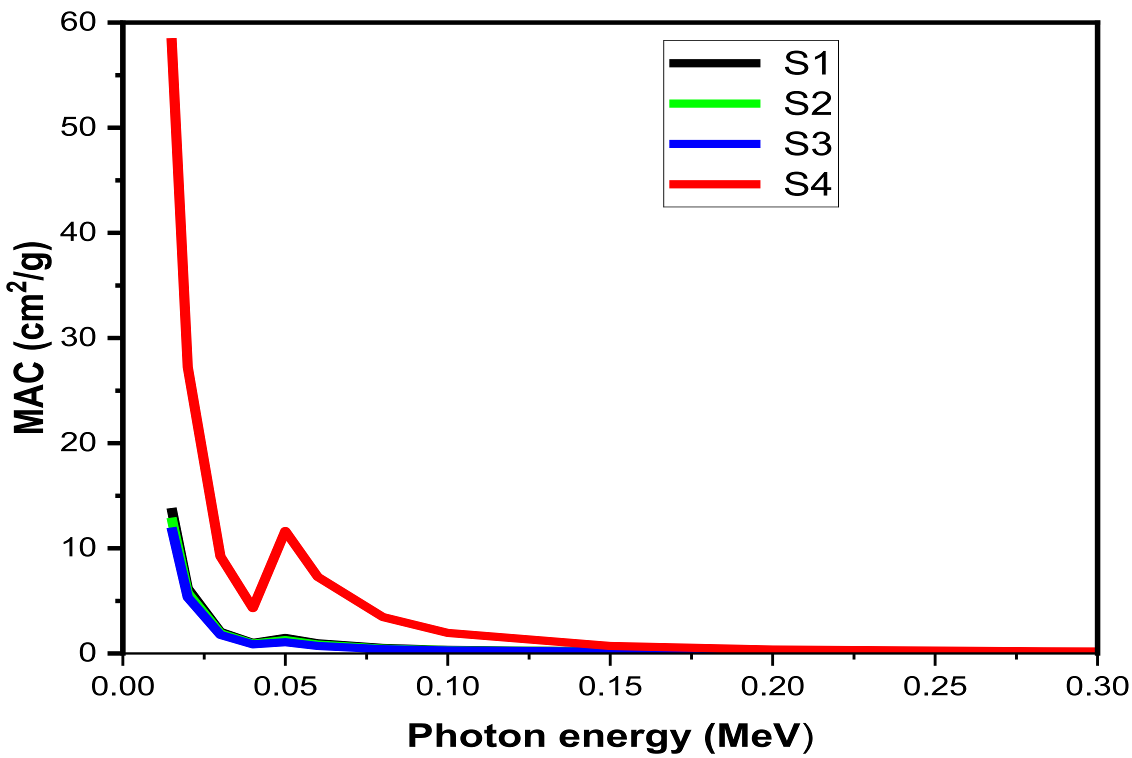

***Fig.* 2: The relationship between photon energy and the mass attenuation coefficient (MAC) in samples**

In another study, the radiation shielding features of heavy metal oxide-based phosphate glasses were investigated. In this study, glass samples with varying compositions of $xPbO_2$ - [(100 - x) (0.5Na_2O - 0.5P_2O_5)] were prepared.

(MAC) increased with higher PbO_2 content and photon energy (from 0.356 to 1.33 MeV).

Linear Attenuation Coefficient (LAC)

The attenuation of the photon intensity emitted from radioactive sources that pass through certain materials can be expressed in terms of the Beer-Lambert law $I = I_0 e^{-\mu t}$. The equation describes the relationship between the initial photon intensity () and the remaining intensity that passes through the medium (I) and demonstrates the medium's ability to block photons passing through it. In the equation, μ represents the linear attenuation coefficient, which is a function of the photon energy and the sample density. A high μ value indicates a sample's ability to block incoming photons (Dong *et al.*, 2019).

In order to estimate the usefulness of the selected S1, S2, S3 and S4 glasses to serve in gamma- radiation shielding applications, which determined by (LAC) of these glasses were determined using Phy-X/PSD at different photon energies. The calculations of LAC were done to signify the shielding ability of the selected samples and to derive the other related shielding factors like the effective atomic number (Zeff) and mean free path (HVL). The results of LAC for S1-S4 glasses versus the energy were tabulated on table 3 and plotted in Fig. 3.

Table 3: LAC values of $20CaSO_4$ + (80-x) P_2O_3 +xSm_2O_3 with 0.50 ≤ x ≤ 2.50 mol % glass system

ENERGY (MeV)	S_1	S_2	S_3	S_4
1.50E-02	43.404	53.233	75.666	182.576
2.00E-02	19.323	23.795	33.938	84.940
3.00E-02	6.396	7.894	11.281	28.803
4.00E-02	3.118	3.833	5.460	13.478
5.00E-02	3.865	5.266	8.120	36.358
6.00E-02	2.578	3.473	5.312	22.740
8.00E-02	1.463	1.915	2.868	10.784
1.00E-01	1.020	1.297	1.899	6.070
1.50E-01	0.636	0.768	1.078	2.235
2.00E-01	0.509	0.599	0.821	1.189
2.84E-01	0.415	0.480	0.647	0.634
3.00E-01	0.403	0.465	0.626	0.582
3.47E-01	0.375	0.431	0.578	0.476
4.00E-01	0.351	0.402	0.537	0.401
5.00E-01	0.316	0.361	0.481	0.320
6.00E-01	0.291	0.332	0.441	0.274
6.62E-01	0.278	0.317	0.421	0.255
8.00E-01	0.254	0.289	0.384	0.223
8.26E-01	0.250	0.284	0.378	0.218
1.00E+00	0.228	0.259	0.344	0.193
1.17E+00	0.210	0.239	0.317	0.175
1.33E+00	0.197	0.224	0.297	0.163
1.50E+00	0.185	0.210	0.279	0.153
2.00E+00	0.160	0.182	0.241	0.134

2.51E+00	0.143	0.163	0.216	0.124
3.00E+00	0.131	0.149	0.199	0.118
4.00E+00	0.115	0.132	0.175	0.111
5.00E+00	0.105	0.121	0.161	0.109
6.00E+00	0.099	0.113	0.151	0.108
8.00E+00	0.091	0.105	0.140	0.110
1.00E+01	0.087	0.100	0.134	0.113
1.50E+01	0.083	0.096	0.129	0.132

The linear attenuation coefficient (LAC), μ\mu, is related to the MAC through the density of the material, according to μ=(μ/ρ)ρ\mu=(\mu/\rho)\rho. Unlike MAC, which is normalized to unit mass, LAC represents attenuation per unit thickness of material.. It is the fraction of photons that interact per unit thickness of attenuating material. Just like MAC, the LAC can be explained based on three absorption mechanisms namely, photoelectric absorption, Compton scattering, and pair production. The variation of LAC (μ) of the $20CaSO_4$ + (80-x)P_2O_3 +xSm_2O_3 with $0.50 \leq x \leq 2.50$ mol % glasses against photon energy (MeV) is illustrated in *Fig.* 3.

The values of LAC at the minimum incident photon energy (E=0.015MeV) where 43.09 cm-1 for (S1), 53.23 cm-1 for (S2), 75.67 cm-1 for (S3) and 182.58cm^{-1} for S4, respectively. Whereas, at the maximum energy (15MeV), the LAC values were found to be 0.085 (S1), 0.096 (S2), 0.129 (S3) and 0.132cm^{-1} for (S4) respectively. The observed rise in LAC at 0.035MeV could be due to a Bi k-absorption edge induced by PE absorption (Liao *et al.*, 2022). Thus, the overall results of the LAC at both minimum and maximum photon energies shows an increase as the content of Sm_2O_3 rises from 0.5 to 2.5 mol%. Eventually, the increase was slowly at Compton and pair production absorption region. The increment of LAC implies that the sample containing a greater amount of Samarium oxide attenuates gamma photons much better compared with those containing less. This trend indicates a strong dependence of LAC on the atomic number of glass materials and the superiority of the S4 glass sample against radiation penetration.

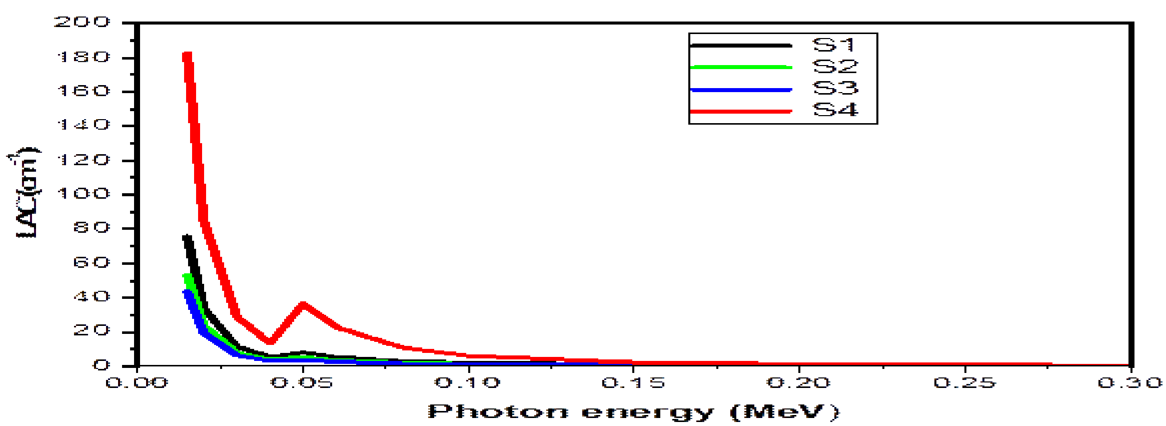

***Fig.* 3: The relationship between photon energy and the Linear attenuation coefficient (LAC) in samples.**

The result of current research agrees with one reported by (Vani *et al*., (2021), in which the effect rare earth dopants on the radiation shielding properties of Barium Tellurite glasses was investigated. Apparently, all the samples have the maximum LAC at 0.245 MeV, the rare earth ions increased the LAC values and the samples with low amount concentration of these rare earth ions have higher LAC than that of the fabricated base sample of Barium Tellurite glass. In another study, gamma ray shielding factors for Barium Phosphate glasses. The Phy-X/PSD software has been used to report the attenuation and penetration factors for this glass system at different energies. The (LAC) values were found to reduce exponentially with increasing the range from 0.176 to 0.496 cm^{-1} (for CaBaP1) and 0.184–0.548 cm^{-1} (for CaBaP6). It was found that the addition of Barium Oxide (BaO) causes an increase in the LAC values from 0.697 to 0.787 cm^{-1} at 0.284 MeV, and from 0.259 to 0.273 cm^{-1} at 0.662 MeV (Al-Hadeethi *et al*., 2020).

Half-Value Layer (HVL)

(HVL) and Tenth Value Layer (TVL) are useful parameters that express a given material's shielding ability against photon energy; they depend on type of photon energy and the composition of the absorbing medium. The HVL and TVL define the thickness of the interacting target at which the attenuated intensities are 90 and 50% of the gamma ray intensity, respectively. The required thickness of the shielding material is inversely proportional to the HVL and TVL values. Therefore, these parameters are important and can be directly derived from LAC (El-khatib *et al.*, 2022).

$$\mathrm{HVL} = 0.693 \times \mathrm{LAC}^{-1}\ (\mathrm{cm}) \quad (2)$$

$$\mathrm{TVL} = 2.303 \times \mathrm{LAC}^{-1}\ (\mathrm{cm}) \quad (3)$$

Table 4: HVL values of $20CaSO_4$ + (80-x) P_2O_3 +xSm_2O_3 with 0.50 ≤ x ≤ 2.50 mol % glass system

ENERGY (MeV)	S_1	S_2	S_3	S_4
1.50E-02	0.016	0.013	0.004	0.009
2.00E-02	0.036	0.029	0.008	0.020
3.00E-02	0.108	0.088	0.024	0.061
4.00E-02	0.222	0.181	0.051	0.127
5.00E-02	0.179	0.132	0.019	0.085
6.00E-02	0.269	0.200	0.030	0.130
8.00E-02	0.474	0.362	0.064	0.242
1.00E-01	0.680	0.534	0.114	0.365
1.50E-01	1.090	0.902	0.310	0.643
2.00E-01	1.362	1.158	0.583	0.845
2.84E-01	1.669	1.444	1.093	1.072
3.00E-01	1.718	1.490	1.191	1.108
3.47E-01	1.846	1.607	1.457	1.200
4.00E-01	1.975	1.724	1.727	1.290
5.00E-01	2.190	1.918	2.165	1.440
6.00E-01	2.384	2.091	2.526	1.572
6.62E-01	2.496	2.190	2.722	1.647
8.00E-01	2.731	2.399	3.111	1.806
8.26E-01	2.774	2.436	3.179	1.835
1.00E+00	3.046	2.678	3.595	2.017
1.17E+00	3.303	2.904	3.965	2.188

1.33E+00	3.526	3.101	4.261	2.337
1.50E+00	3.746	3.294	4.532	2.483
2.00E+00	4.336	3.811	5.157	2.872
2.51E+00	4.852	4.262	5.590	3.210
3.00E+00	5.285	4.639	5.882	3.491
4.00E+00	6.009	5.267	6.226	3.958
5.00E+00	6.570	5.750	6.368	4.314
6.00E+00	7.005	6.122	6.404	4.587
8.00E+00	7.607	6.631	6.313	4.956
1.00E+01	7.973	6.935	6.138	5.173
1.50E+01	8.377	7.257	5.674	5.392

The variation of the HVL parameter of the glass samples under investigation with respect to incident photon energy was illustrated in Figs. 4. T. The HVL generally increases with increasing photon energy, (from 0.015MeV to 7MeV) reflecting the corresponding decrease in LAC.

Furthermore, as the Sm content changes from low to higher (1 – 2.5mol %), the HVL reduces, thereby maximizing the chances of photon interaction with the glass material. Notably, in the photon energy range of 15keV ≤ E≤ 70keV, the values demonstrate a gradual decrement as the Samarium content changes progressively. Sample S4 has a value of 0.009 cm for HVL at E=15keV. Similarly, when E=15MeV, the values are 5.392cm for HVL. When considering the sample with low concentration of Sm, (S1) has the values of 0.016 cm for HVL at E=15keV whereas, at E=15MeV, the values are 8.377 cm. Careful inspection indicates that the sample containing low Samarium concentration has a higher value of HVL, respectively. Conversely, low values of HVL were illustrated by samples with high samarium content. This behavior generally indicates addition of Samarium into the studied glass system modifies their shielding ability, and sample S4 has superb photon attenuation capacity when compared to other samples with low Samarium levels.

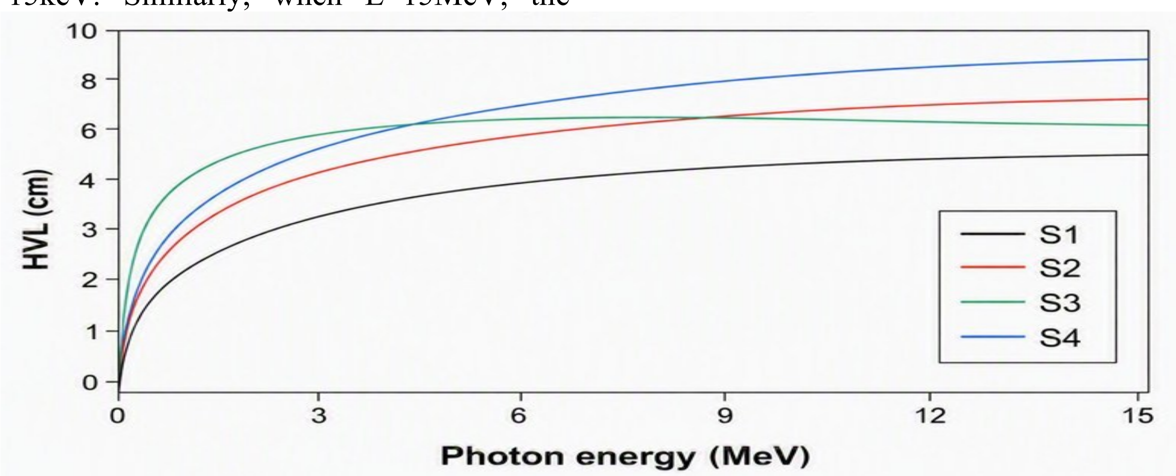

***Fig.* 4: The relationship between photon energy and the Half value layer (HVL) in samples.**

Mean Free Path (MFP)

MFP ;- travelled by photons between two successive interactions. It is the most significant parameter that directly interprets the ability of any barrier to reduce the gamma radiations. It has been reported in past that material with lower value of MFP has good shielding efficiency. (MFP) represents the average distance travelled by an incident γ-ray photon before interacting with the attenuating material (i.e., the glass system). MFP is typically defined in terms of LAC, as expressed in equation (4). $MFP = LAC^{-1}$ (cm) (4)

Table 5: MFP values of $20CaSO_4 + (80-x) P_2O_3 + xSm_2O_3$ with $0.50 \leq x \leq 2.50$ mol % glass system

ENERGY (MeV)	S_1	S_2	S_3	S_4
1.50E-02	0.013	0.019	0.023	0.005
2.00E-02	0.029	0.042	0.052	0.012
3.00E-02	0.089	0.127	0.156	0.035
4.00E-02	0.183	0.261	0.321	0.074
5.00E-02	0.123	0.190	0.259	0.028
6.00E-02	0.188	0.288	0.388	0.044
8.00E-02	0.349	0.522	0.684	0.093
1.00E-01	0.527	0.771	0.981	0.165
1.50E-01	0.928	1.301	1.572	0.447
2.00E-01	1.219	1.670	1.965	0.841
2.84E-01	1.547	2.084	2.408	1.576
3.00E-01	1.598	2.149	2.479	1.718
3.47E-01	1.731	2.319	2.664	2.101
4.00E-01	1.862	2.487	2.849	2.492
5.00E-01	2.077	2.767	3.160	3.123
6.00E-01	2.267	3.016	3.439	3.644
6.62E-01	2.377	3.159	3.600	3.928
8.00E-01	2.606	3.461	3.940	4.489
8.26E-01	2.647	3.515	4.002	4.586
1.00E+00	2.910	3.863	4.395	5.187
1.17E+00	3.157	4.189	4.765	5.720
1.33E+00	3.372	4.474	5.087	6.148
1.50E+00	3.582	4.752	5.404	6.538
2.00E+00	4.144	5.499	6.255	7.440
2.51E+00	4.631	6.149	7.000	8.065
3.00E+00	5.037	6.693	7.624	8.485
4.00E+00	5.710	7.599	8.670	8.982
5.00E+00	6.224	8.296	9.479	9.188
6.00E+00	6.617	8.832	10.106	9.239
8.00E+00	7.150	9.566	10.974	9.107
1.00E+01	7.463	10.006	11.503	8.855
1.50E+01	8.779	10.470	12.086	8.186

The MFP as a function of photon energy of the glasses under investigation shows in *Fig.* 5. The values at minimum energy (E=15keV), the values were 0.013 (S1), 0.019 (S2), 0.023 (S3) and 0.005 cm (S4). Similarly, at 15MeV, the values of MFP for the four samples are 8.779, 10.470, 12.86 and 8.186cm, respectively. The outcome of their results indicated that the glass sample S4 recorded the least values across all the studied energy intervals. This emphasizes the quality and potentiality of utilizing S4 glass for shielding ionizing radiation.

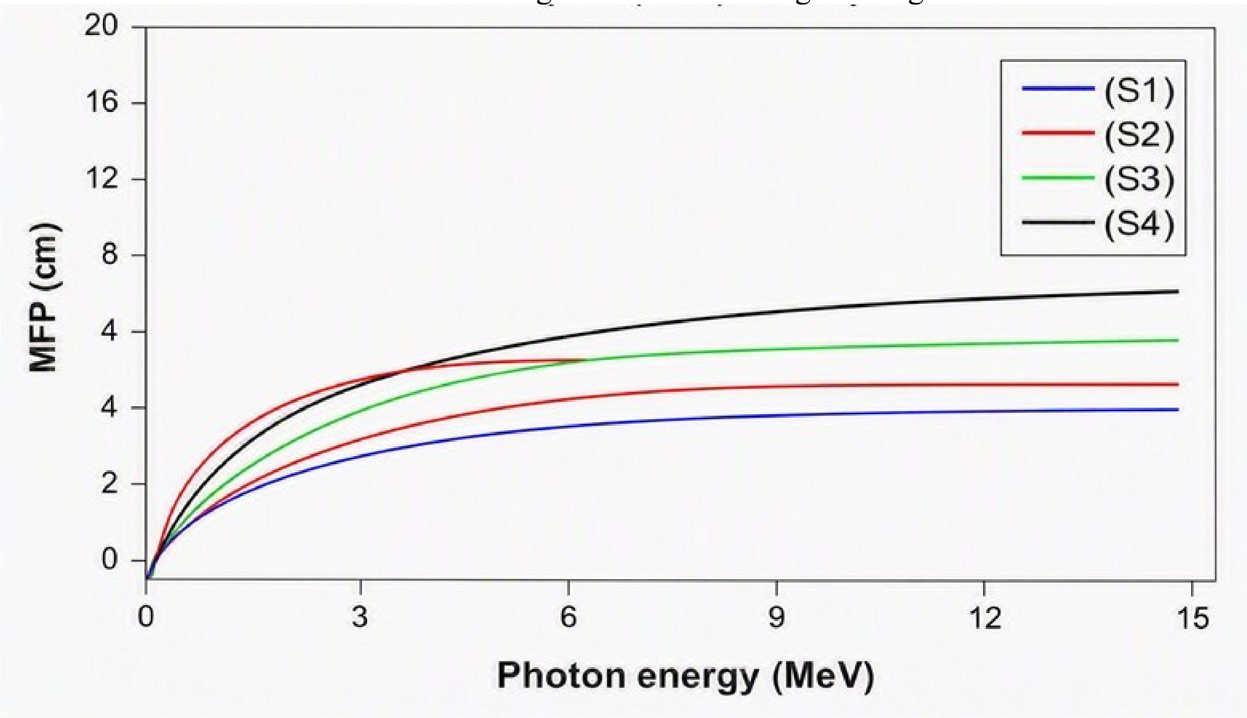

Fig. 5: The relationship between photon energy and the mean free path (MFP) in samples.

Table 6: (Z_{eff}) values of $20CaSO_4 + (80-x) P_2O_3 + xSm_2O_3$ with $0.50 \leq x \leq 2.50$ mol % glass system

ENERGY (MeV)	S_1	S_2	S_3	S_4
3.47E-01	11.96	11.76	11.56	27.90
4.00E-01	11.81	11.64	11.47	26.16
5.00E-01	11.65	11.51	11.37	24.17
6.00E-01	11.57	11.44	11.32	23.07
6.62E-01	11.54	11.42	11.30	22.62
8.00E-01	11.49	11.38	11.27	21.95
8.26E-01	11.49	11.38	11.26	21.86
1.00E+00	11.46	11.35	11.25	21.42
1.17E+00	11.44	11.34	11.24	21.16
1.33E+00	11.44	11.33	11.23	21.07
1.50E+00	11.44	11.34	11.23	21.06
2.00E+00	11.47	11.36	11.26	21.34
2.51E+00	11.52	11.41	11.30	21.87
3.00E+00	11.58	11.46	11.34	22.45
4.00E+00	11.71	11.57	11.44	23.69

5.00E+00	11.84	11.69	11.54	24.89
6.00E+00	11.97	11.80	11.64	25.98
8.00E+00	12.20	12.01	11.82	27.85
1.00E+01	12.41	12.19	11.98	29.35
1.50E+01	12.80	12.54	12.28	31.99

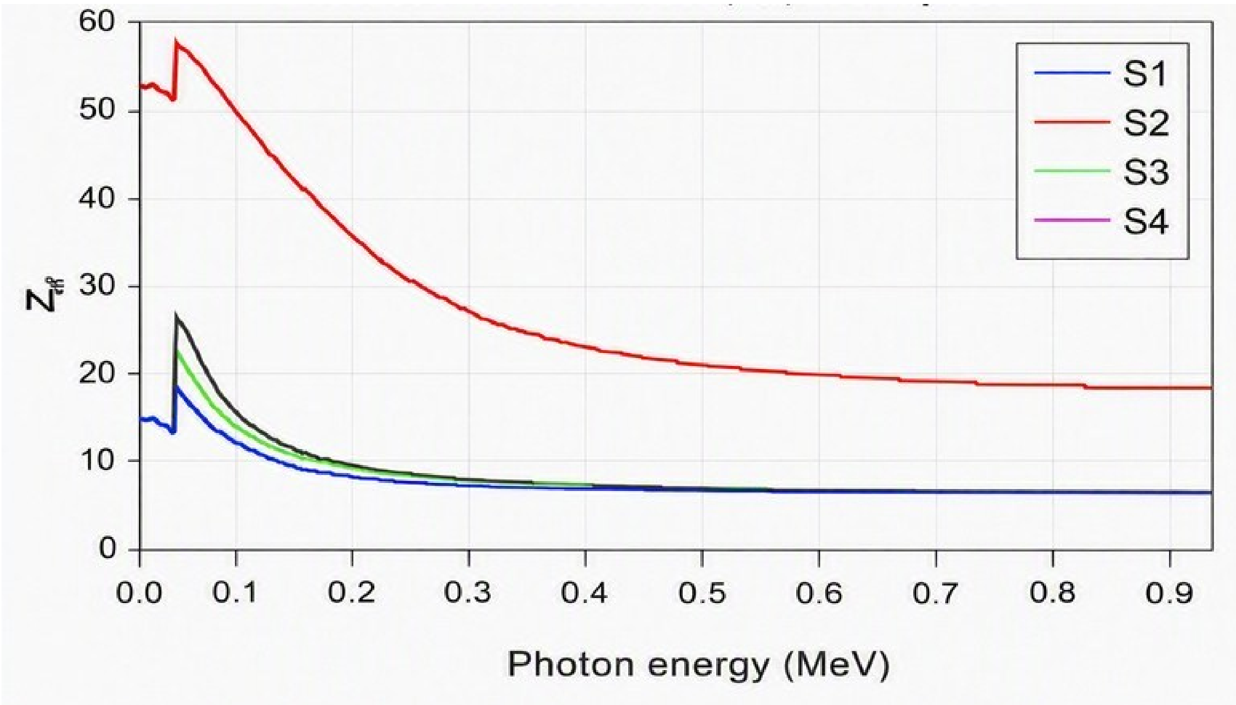

Fig. 6: The relationship between photon energy and Effective Atomic Number (Z_{eff}) in samples.

Effective Atomic Number (Z_{eff})

Another photon interaction parameter that can be obtained from LAC values and are frequently used to understand the effects of the composition on the photons attenuation features is denoted by the effective atomic number (Z_{eff}). The higher Z_{eff} values for a glass system imply that it is more able to block the radiation. Table 6 illustrate Zeff variation with the photon energy for all the prepared glasses samples over the energy ranges (0.015 to 15 MeV).

The values at minimum energy (E=15keV), the values for Z_{eff} were 11.96 (S1), 11.76 (S2), 11.56 (S3) and 27.90 (S4). Similarly, at 15MeV, the values of Z_{eff} for the four samples were 12.80, 12.54, 12.28 and 31.99, respectively. The Z_{eff} is in agreement with the findings of (Yalcin *et al.*, 2019).

The fluctuation in Z_{eff} can be clarified via three distinct photon interaction mechanisms (PP, CS, and PE) at low, intermediate, and high energy regions. At low energy, the maximum value of Z_{eff} is found because the PE cross section is the predominant process determined strongly atomic number of the material (Z^4). The minimum Z_{eff} value is attained in the intermediate energy zone dominated by the CS cross section. However, in the region of high energy, the values of Z_{eff} manifest increase due to the dominance of the PP cross section, which has a weaker Z^2 atomic number of the material (Z^2) dependence. It is worth mentioning that materials with higher Z_{eff} values have the highest probability of photon interaction and better photon attenuation. Conclusively, the value Z_{eff} for S4 glass appears to be higher than S1–S3, which indicates its supremacy in stopping/shielding incoming gamma energies.

4.0 Conclusion

Some important radiation shielding parameters such as MAC, LAC, MFP, HVL and effective atomic number (Z_{eff}) of the glass with composition $20CaSO_4 + (80\text{-}x)P_2O_3 + xSm_2O_3$ with $0.50 \leq x \leq 2.50$ mol % have been calculated using the Phy-X/PSD software. The investigated glasses exhibit an increasing trend of the MAC with varying amounts of Sm_2O_3 in the order of $S1 > S2 > S3 > S4$. The observed increase in density of the prepared samples (Table 1) correlates with the increasing value of the MAC. Convincingly, the sample S4 demonstrates superior radiation attenuation efficiency based on its high MAC compared to S1, S2 and S3 samples.

The values of LAC at the minimum incident photon energy (E=0.015MeV) were 43.09 (S1), 53.23 (S2), 75.67 (S3) and 182.58cm^{-1} for S4, respectively. Whereas, at the maximum energy (15MeV), the LAC values were found to be 0.085 (S1), 0.096 (S2), 0.129 (S3) and 0.132cm^{-1} for (S4) respectively. The observed rise in LAC at 0.035MeV could be due to a Bi k-absorption edge induced by PE absorption. Thus, the overall results of the LAC at both minimum and maximum photon energies show an increase as the content of Sm_2O_3 rises from 0.5 to 2.5 mol%. Eventually, the increase was slowly at Compton and pair production absorption region. The increment of LAC implies that the sample containing a greater amount of samarium oxide attenuates gamma photons much better compared with those containing less. This trend indicates a strong dependence of LAC on the atomic number of glass materials and the superiority of the S4 glass sample against radiation penetration.

The variation of the HVL parameter of the glass samples under investigation with respect to incident photon energy. The values of HVL increases with an increment in photon energy from 0.015MeV to 7MeV and then decrease above 7MeV. Furthermore, as the Sm content changes from low to higher (1 – 2.5mol%). This behavior generally indicates addition of Samarium into the studied glass system modifies their shielding ability, and sample S4 has superb photon attenuation capacity when compared to other samples with low Samarium levels.

The MFP as a function of photon energy was investigated. The values at minimum energy (E=15keV), the values were 0.013 (S1), 0.019 (S2), 0.023 (S3) and 0.005 cm (S4). Similarly, at 15MeV, the values of mfp for the four samples are 8.779, 10.470, 12.86 and 8.186cm, respectively. The outcome of their results indicated that the glass sample S4 recorded the least values across all the studied energy intervals. This emphasizes the quality and potentiality of utilizing S4 glass for shielding ionizing radiation. The results showed the possibility of use the studied glasses for the radiation shielding applications.

5.0 References

Abdelhakim, N. A., Shalaby, R. M., Abdelghany, A. M., Mitwalli, M., El-Farrash, A. H., & Saleh, A. (2026). Integration between radiation shielding performance, structural evolution, and mechanical features of co-doped sodium phosphate glasses. *Scientific Reports*, 16, 1, Article 1958. https://doi.org/10.1038/s41598-025-33307-w

Abouhaswa, A. S., Sayyed, M. I., Altowyan, A. S., Al-Hadeethi, Y., & Mahmoud, K. A. (2021). Synthesis, optical and radiation shielding capacity of the Sm2O3 doped borate glasses. *Journal of Non-Crystalline Solids*, 553, 120505. https://doi.org/10.1016/j.jnoncrysol.2020. 120505

Akram, S., & Chowdhury, Y. S. (2023). Radiation exposure of medical imaging. In StatPearls. StatPearls Publishing.

http://www.ncbi.nlm.nih.gov/books/ NBK 565909/

Al-Hadeethi, Y., & Sayyed, M. I. (2020). A comprehensive study on the effect of TeO2 on the radiation shielding properties of TeO2–B2O3–Bi2O3–LiF–SrCl2 glass system using Phy-X / PSD software. *Ceramics International*, 46, 5, pp. 6136–6140. https://doi.org/10.1016/j.ceramint.2019.11.078

Arul Raja Sekaran, S., Naseer, K. A., Marimuthu, K., Almousa, N., & Sayyed, M. I. (2024). Investigations on physical, structural, elastic, optical and radiation shielding properties of calcium phospho-silicate glasses. *Radiation Physics and Chemistry*, 214, Article 111306. https://doi.org/10.1016/j.radphyschem.2023.111306

Auwal, Y. M., Livinius, E. A., & Ali, W. (2022). *Dose rate and cancer risk simulation from natural radioactivity concentration in Lamja Coal Mine's, Adamawa-Nigeria*. August. https://doi.orgb/10.1002/acm2.137872

Auwal, Y. M., & Pascal, T. (2025). Health risk assessment of indoor radon exposure in some residential dwellings across North East, Nigeria. 11, 2, pp. 211–225.

Auwal, Y. M., Meludu, O. C., & Pascal, T. (2025). *Computational modeling and validation of indoor radon gas dynamics and accumulation using Ansys Fluent Simulation* 2025. 12, April, pp. 1172–1183.

Aliyu, A. M., & Ahmed, N. E. (2019). Structure and physical properties of 30MgSO4-(70-x)P2O5-xSm2O3 glasses. EDUCATUM *Journal of Science, Mathematics and Technology*, 6, 2, Article 2. https://doi.org/10.37134/ejsmt. vol6.2.3 . 2019

Barde, M. M., Aliyu, A. M., Baballe, A., & Iliyasu, A. S. (2026). Studies of the properties of calcium sulfate ultra-phosphate glasses doped dyprosium for ionizing radiation shielding applications. *BIMA Journal of Science and Technology* Gombe, 10, 1A, pp. 240–250. https://doi.org/10.64290/bima.v10i1 A. 1538

Barman, R., Hossain, Md. S., Das, A., & Ahmmad Rabby, Md. K. (2022). Investigation of radiation shielding characteristic features of different wood species. *Radiation Physics and Chemistry*, 192, 109927. https://doi.org/10.1016/j.radphyschem.2021.109927

Dong, M. G., Xue, X. X., Elmahroug, Y., Sayyed, M. I., & Zaid, M. H. M. (2019). Investigation of shielding parameters of some boron containing resources for gamma ray and fast neutron. *Results in Physics*, 13, 102129. https://doi.org/10.1016/j.rinp.2019.02.065

El-khatib, Ahmed M., Abbas, M. I., Sayyed, M. I., Khandaker, M. U., Abd-Elzaher, M., Khalil, M. M., Elsafi, M., & Gouda, M. M. (2022). Assessment of γ-radiation shielding behavior of some mixed nature clays. *Radiation Physics and Chemistry,* 200, 110236. https://doi.org/10.1016/j.radphyschem.2022.110236

Frane, N., & Bitterman, A. (2023). Radiation safety and protection. In StatPearls. StatPearls Publishing. http://www.ncbi.nlm.nih.gov/ books/NBK 557499/

Geidam, I. G., Matori, K. A., Halimah, M. K., Chan, K. T., Muhammad, F. D., Ishak, M., & Umar, S. A. (2022). Oxide ion polarizabilities and gamma radiation shielding features of TeO2–B2O3–SiO2 glasses containing Bi2O3 using Phy-X/PSD software. *Materials Today Communications*, 31, 103472. https://doi.org/10.1016/j.mtcomm.2022.103472

Hanfi, M. Y., Sakr, A. K., Ismail, A. M., Atia, B. M., Alqahtani, M. S., & Mahmoud, K. A. (2023). Physical characterization and radiation shielding features of B2O3–

As2O3 glass ceramic. *Nuclear Engineering and Technology*, 55, 1, pp. 278–284. https://doi.org/10.1016/j.net.2022.09.006

Hila, F. C., Sayyed, M. I., Javier-Hila, A. M. V., & Jecong, J. F. M. (2022). Evaluation of the radiation shielding characteristics of several glass systems using the EPICS2017 library. *Arabian Journal for Science and Engineering*, 47, 1, pp. 1077–1086. https://doi.org/10.1007/ s13369-021-06062-z

Ige, O. A. (2023). *Sources of recycled aggregates for concrete production. In Y. Xu & R. Jin (Eds.), Multi-Functional Concrete with Recycled Aggregates* (pp. 3–16). Woodhead Publishing. https://doi.org/10.1016/B978-0-323-89838-6.00002-5

Jeng, R.-J., Kishi, T., Matsushita, N., & Yano, T. (2019). Optical bonding of tellurite glass film on silicate glass. *International Journal of Applied Glass Science*, 10, 2, pp. 248–258. https://doi.org/10.1111/ijag.13094

Kim, J. H. (2018). Three principles for radiation safety: Time, distance, and shielding. *The Korean Journal of Pain*, 31, 3, pp. 145–146. https://doi.org/10.3344/kjp.2018.31.3.145

Kumar, A., Chakrabarti, A., Shekhawat, M. S., & Molla, A. R. (2019). Transparent ultra-low expansion lithium aluminosilicate glass-ceramics: Crystallization kinetics, structural and optical properties. *Thermochimica Acta*, 676, pp. 155–163. https://doi.org/10.1016 /j.tca.2019.04.006

Liao, W., Zhang, X., Ke, S., Shao, J., Yang, H., Zhang, S., & Chen, H. (2022). Effect of different biomass species and pyrolysis temperatures on heavy metal adsorption, stability and economy of biochar. *Industrial Crops and Products*, 186, 115238. https://doi.org/10.1016/j.indcrop.2022.115238

More, C. V., Alsayed, Z., Badawi, Mohamed. S., Thabet, Abouzeid. A., & Pawar, P. P. (2021). Polymeric composite materials for radiation shielding: A review. *Environmental Chemistry Letters*, 19, 3, pp. 2057–2090. https://doi.org/10.1007/s10311-021-01189-9

Mortazavi, S. M. J., Bevelacqua, J. J., Rafiepour, P., Sina, S., Moradgholi, J., Mortazavi, A., & Welsh, J. S. (2024). *Chapter 13—Lead-free, multilayered, and nanosized radiation shields in medical applications, industrial, and space research. In S. Verma & A. K. Srivastava (Eds.), Advanced Radiation Shielding Materials* (pp. 305–322). Elsevier. https://doi.org/10.1016/B978-0-323-5387-0.00006-6

Park, H., Paganetti, H., Schuemann, J., Jia, X., & Min, C. H. (2021). Monte Carlo methods for device simulations in radiation therapy. *Physics in Medicine and Biology*, 66, 18. https://doi.org/10.1088/1361-6560/ac1 d1f

Qian, Z., Cai, J., Li, C., Zhang, Z., & Wang, J. (2021). Influence of PbO content on the gamma ray shielding properties of lead boro-telluro-phosphate glasses. *Radiation Physics and Chemistry*, 185, 109516. https://doi.org/10.1016/j.radphyschem.2021.109516

Rammah, Y. S., Mahmoud, K. A., Sadeq, M. S., Haily, E., Bih, L., Ahmed, E. M., & El-Agawany, F. I. (2022). Optical and radiation shielding properties of titano-phosphate glasses: Influence of BaO. *Journal of the Australian Ceramic Society*, 58, 3, pp. 867–880. https://doi.org/10.1007/s41779-022-007 34-1

Saddeek, Y. B., Issa, S. A. M., Alharbi, T., Elsaman, R., Abd elfadeel, G., Mostafa, A. M. A., Aly, K., & Ahmad, M. (2020). Synthesis and characterization of lead borate glasses comprising cement kiln dust and Bi2O3 for radiation shielding protection. *Materials Chemistry and Physics,* 242, 122510. https://doi.org/10.1016/j.matchemphys. 2019.122510

Sayyed, M. I. (2017). Half value layer, mean free path and exposure buildup factor for tellurite glasses with different oxide compositions. *Journal of Alloys and Compounds*, 695, pp. 3191–3197. https://doi.org/10.1016/j.jallcom. 2016.11.318

Sayyed, M. I., Tekin, H. O., & Agar, O. (2019). Gamma photon and neutron attenuation properties of MgO–BaO–B2O3–TeO2–Cr2O3 glasses: The role of TeO2. *Radiation Physics and Chemistry*, 163, pp. 58–66. https://doi.org/10.1016/j.radphyschem.2019.05.012

Sivasankara Reddy, N. (2022). Role of zinc sulfate on thermal and mechanical properties of borovanadate glasses. *Materials Today*: *Proceedings*, 49, pp. 771–776. https://doi.org/10.1016/j.matpr. 2021.05.292

Vani, P., Vinitha, G., Sayyed, M. I., AlShammari, M. M., & Manikandan, N. (2021). Effect of rare earth dopants on the radiation shielding properties of barium tellurite glasses. *Nuclear Engineering and Technology,* 53, 12, pp. 4106–4113. https://doi.org/10.1016/j.net. 2021.06.009

Yalcin, S., Aktas, B., & Yilmaz, D. (2019). Radiation shielding properties of Cerium oxide and Erbium oxide doped obsidian glass. *Radiation Physics and Chemistry*, 160, pp. 83–88. https://doi.org/10.1016/j.radphy schem.2019.03.024

Zaynal, S. A., Ülgen, P. N., Eken, S., Şahin, M. C., & Manisa, K. (2026). Investigation of radiation shielding properties of samarium oxide doped photopolymer composites for additive manufacturing applications. *AJEAS*, 4, 1, pp. 1–9. http://dx.doi.org/10.70988/ajeas.1911344

Zhang, X., Wang, Y., Wu, X., Wang, F., Ou, Q., & Zhang, S. (2024). A comprehensive review on mechanisms and applications of rare-earth based perovskite nanocrystals. *Chinese Journal of Chemistry*, 42, 9, pp. 1032–1056. https://doi.org/10.1002/cjoc.202300344

Declaration:

Consent for publication

Not Applicable

Data Availability Statement:

The datasets supporting the findings of this study are available in the manuscripts

Conflict of Interest

Not Applicable

Ethical Considerations

Not applicable

Funding

The author(s) declared no source of funding

Authors' Contributions

Tanimu Hussaini and Sadiq Abubakar Dalhatu conceived the study and designed the methodology. Dauda Abubakar,Auwal Baballe, Haruna Saleh, Yawale Abubakar Ibrahim, Mohammed Rabiu, and Nafisa Musa contributed to data collection, analysis, and interpretation. Yusuf Mohammed Auwal contributed to supervision, manuscript review, and editing. All authors read and approved the final manuscript.